ELSEVIER

Journal of Power Sources 102 (2001) 105–111

JOURNAL OF POWER SOURCES

www.elsevier.com/locate/jpowsour

# Influence of zinc on the stability of the β(II)/β(III) nickel hydroxide system during electrochemical cycling

Cécile Tessier[a,b], Liliane Guerlou-Demourgues[a], Christiane Faure[a], Catherine Denage[a], Bruno Delatouche[a], Claude Delmas[a,*]

[a]*Institut de Chimie de la Matière Condensée de Bordeaux, CNRS and Ecole Nationale Supérieure de Chimie et Physique de Bordeaux, 87 Av. Dr. A. Schweitzer, 33608 Pessac Cedex, France*

[b]*SAFT, Direction de la Recherche, 111-113 Boulevard Alfred Daney, 33074 Bordeaux Cedex, France*

Received 26 April 2000; received in revised form 20 March 2001; accepted 27 March 2001

**Abstract**

The present paper aims at discussing efficiency tests, which particularly examine the response on discharge to an increasing charge duration, in a galvanostatic mode, for β(II)-type zinc-substituted nickel hydroxides. The influence of a preliminary formation of the materials in a low-concentration electrolyte is underlined and the effect of zinc on the inhibition of the transformation of the β(III)-phase into the γ-one is also demonstrated. It is shown that the presence of zinc increases the cell voltage as a result of the large size of zinc ions as compared to nickel ions. 

*Keywords:* Nickel hydroxide; Zinc–nickel hydroxide; Alkaline batteries; Nickel hydroxide electrode

## 1. Introduction

Nickel hydroxide has been the subject of many studies because of its use as an active material in alkaline batteries. Several elements are commonly substituted for nickel in order to improve its electrochemical behaviour in commercial batteries. Recently zinc was substituted for nickel, especially for Ni/MH batteries, since studies reported its capacity to prevent the formation of the γ-phase on charge [1–7].

An intensive study of zinc-substituted nickel hydroxides was recently carried out in our lab. The structural investigation demonstrated that a β(II)-type phase is formed with up to 15% zinc [8]. During ageing tests in KOH, an Oswald ripening occurs [9], with a loss of zinc in the solution [10]. The redox reactions occur in the solid state, and in this case, a partial loss of zinc is also observed, but only during the β(III) → γ transformation upon overcharge. Because all these processes occur simultaneously during the electrochemical cycling, the electrochemical behaviour is very complex, as shown in a recent study [11]. The γ-phase is formed on charge during the first cycles, followed by an evolution to the β(II)/β(III) system, leading to a long-term stable capacity. Fig. 1 shows the evolution of the number of exchanged electrons per nickel atom (NEE/Ni) for a β(II)-phase with 6% zinc in substitution for nickel, (denoted $\beta_{6\%\ Zn}$), as compared to that of a phase without zinc ($\beta_{0\%\ Zn}$), during a galvanostatic cycling test in a 8 M KOH electrolyte at the *C*/5 rate. It clearly highlights the increase in the capacity exchanged per nickel atom in the presence of zinc. In the work reported in [11], the processes involved in the transition from the α/γ system back to the β(II)/β(III) one, after the initial formation of the γ-phase on charge were highlighted. Moreover, it was shown that during cycling tests in electrolytes with various concentrations (increasing from 2 to 4, 6 and 8 M), the presence of zinc delays the formation of the γ-phase on charge.

The present work concerns β(II)-type zinc-substituted nickel hydroxides containing 0–15% zinc and deals with the influence of zinc on the transformation of β(III) to γ, on charge, during a galvanostatic cycling in 8 M KOH, when the charge duration is increased after each cycle. In the present paper, this experiment is called an efficiency test. This study is complementary to that previously reported [11]. Two kinds of experiments were carried out: one of them includes a preliminary electrode formation process before the efficiency test, whereas, in the other one, the efficiency test is directly performed without any preliminary formation of the electrode.

* Corresponding author. Tel.: +33-5-5684-6296; fax: +33-5-5684-6634.
*E-mail address*: delmas@icmcb.u-bordeaux.fr (C. Delmas).

0378-7753/01/$ – see front matter 
PII: S0378-7753(01)00799-6

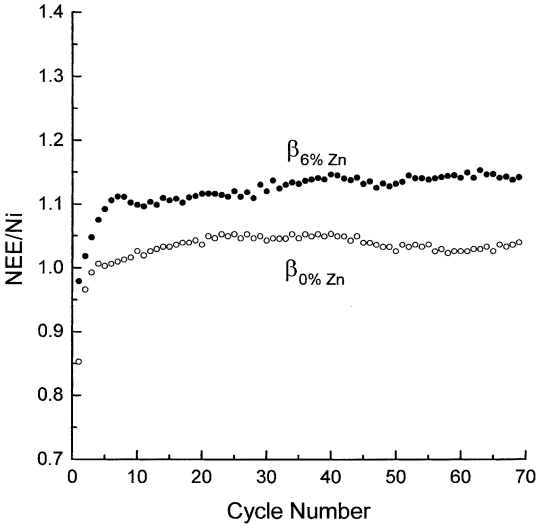


Fig. 1. Variation of the NEE/Ni, at the *C*/5 rate, in 8 M KOH electrolyte, as a function of the cycle number, for the $\beta_{0\%\ Zn}$ and $\beta_{6\%\ Zn}$ phases.

## 2. Experimental

Zinc-substituted nickel hydroxides were obtained by precipitation: 200 ml of a 1 M metal salt solution ($NiSO_4$ and $ZnSO_4$ in the appropriate ratio) were dropped into 300 ml of a 2 M NaOH solution. The pH value was thus maintained equal to 14 throughout the precipitation. The precipitate was then washed with deionised water, until the washing water reached a steady pH equal to 8–9, before being dried for 15 h at 90°C.

Electrodes for electrochemical tests were prepared by mixing 2/3 in weight of the active material with 1/3 of graphite to ensure a good electronic conductivity. An amount of 1 wt.% of powdered polytetrafluoroethylene was then added in order to increase the mechanical strength and the resulting mixture was pasted onto a nickel foam (1 cm × 5 cm size). The whole electrode was pressed at 1 Torr/cm$^2$ and placed into a non-woven tissue and then positioned between two polyvinyl chloride plates. Two sintered cadmium hydroxide electrodes were placed on both sides of the positive electrode, their capacity strongly exceeding that of the positive electrode, so as not to limit the cycling of the battery. In the following, all the potential values are given versus $Cd(OH)_2$/Cd.

All the experiments were carried out in a galvanostatic mode. Some efficiency tests were preceded by a formation process, which was performed in a 1 M KOH electrolyte. This consists in a first charge lasting 20 h at the *C*/10 rate, meaning that the value of the current intensity is such that 10 h are required to exchange one electron per (nickel + zinc) atom. The subsequent discharge as well as the following cycles were performed at the *C*/5 rate, with 6 h long charges and discharges down to 0.9 V. The proper efficiency test was performed in an 8 M KOH electrolyte, at the *C*/5 rate, with a charge duration increasing cycle after cycle and discharges down to 0.9 V. The first charge imposed on the battery lasted 60 min, followed by charges ranging from 120 to 240 min, with a 30 min step, and from 240 to 450 min, with a 15 min step.

The X-ray diffraction patterns (XRD) were obtained on a Siemens D5000 diffractometer (Cu Kα) with a scan step of 0.04° (2$\theta$) for 40 s.

## 3. Results and discussion

The electrochemical behaviour of the $\beta_{10\%\ Zn}$ and $\beta_{15\%\ Zn}$ materials was investigated both with and without preliminary electrode formation and compared to that of a non-substituted β-phase ($\beta_{0\%\ Zn}$) cycled in the same conditions. The variations of the NEE per nickel ion are presented in Figs. 2 and 3 for the various materials. Several electrodes were systematically tested for each zinc composition and led to quite similar results. For the sake of clarity only one curve per zinc amount, representative of the average behaviour, is presented in the figures.

It is useful to relate the evolution of the capacities to that of the corresponding derivatives of the discharge curves. Indeed, these derivatives indicate the various redox systems involved in the discharge reaction. A two-phase redox system is characterised by a plateau (or a pseudo-plateau) in the potential versus time curve, which leads to a peak in the derivative of time versus potential curve, so that this derivative is very often easier to handle. Derivative curves have already been used to discriminate between the involvement in the cycling of the α/γ or β(II)/β(III) system, for

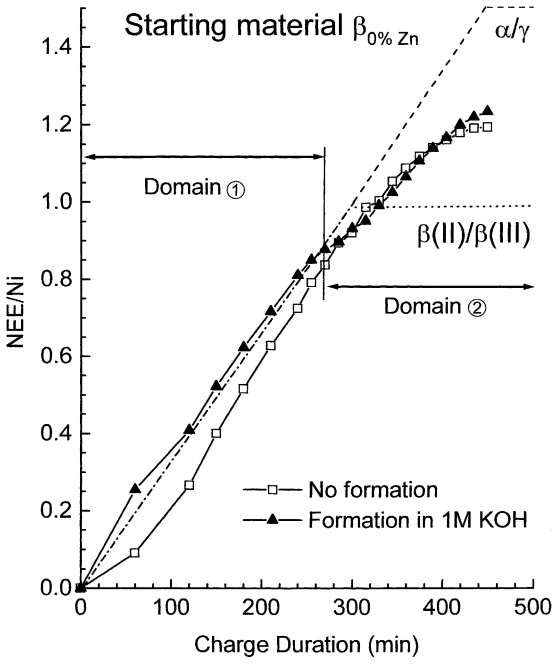


Fig. 2. Variation of the NEE/Ni as a function of charge duration, during a galvanostatic efficiency test, carried out either with electrode formation (▲) or without electrode formation (□), starting from a $\beta_{0\%\ Zn}$-phase (see text for details).

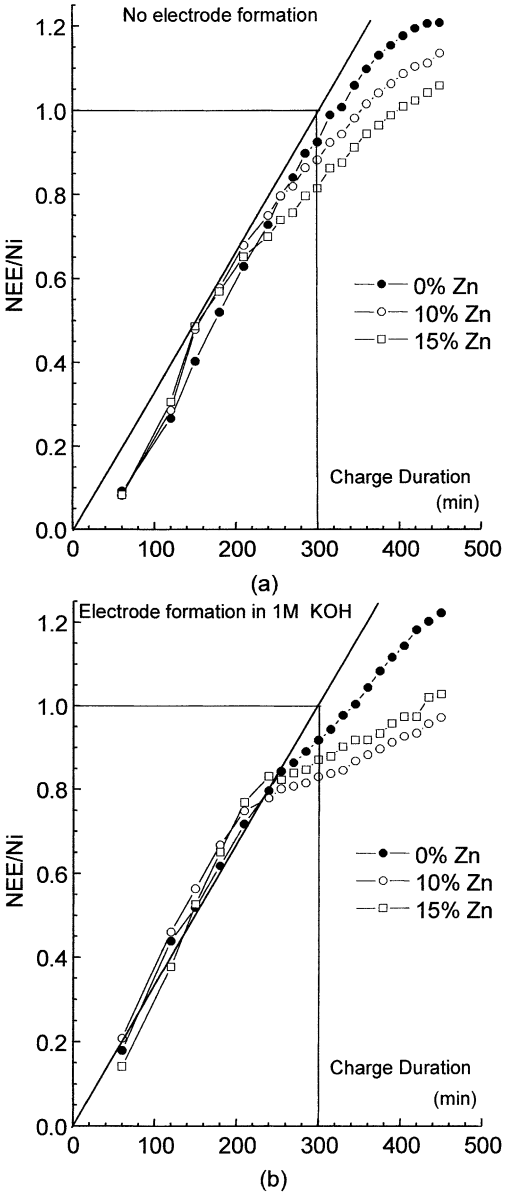


Fig. 3. Variations of the NEE/Ni as a function of charge duration, during galvanostatic efficiency tests carried out for the $\beta_{0\%\ Zn}$, $\beta_{10\%\ Zn}$ and $\beta_{15\%\ Zn}$ phases either without (a) or with (b) preliminary electrode formation.

instance in the case of non-substituted nickel hydroxides [12], of manganese-substituted nickel hydroxides [13] or to investigate the second discharge plateau [14]. These derivative curves give the same information as the voltammograms commonly used by electrochemists. The evolutions of the discharge derivative curves with increasing charge duration are shown in Fig. 4 for the $\beta_{0\%\ Zn}$, $\beta_{10\%\ Zn}$ and $\beta_{15\%\ Zn}$ phases, studied both with and without preliminary formation. Whatever the zinc amount, two kinds of contributions can be distinguished in all curves: one rather sharp peak centred in the 1.16–1.18 V domain and a second peak, much wider, which extends over the 1.21–1.25 V range. A study of the zinc-substituted β(II)-phase, reported in a previous paper, led us to conclude that the former peak is due to the α/γ system while the latter corresponds to the β(II)/β(III) one [11]. These attributions correlate with the potential values suggested by Barnard for the two systems [15]. It should be noted that, in a previous paper, the significant width of the contribution attributed to the β(II)/β(III) system was correlated with the presence of several β(II)-type phases that exhibit different structural features, such as octahedral vacancies within the slab or zinc in the interslab space. Those different β(II)-type phases may lead to different redox potentials resulting in a rather wide peak [11].

### 3.1. Behaviour of the $\beta_{0\%\ Zn}$-phase

A comparison of the two curves corresponding to the evolution of the capacity with or without formation in the case of the non-substituted β(II)-phase (Fig. 2) leads to general tendencies which will be extended to the zinc-substituted phases.

The dotted and dashed lines correspond to the theoretical curves obtained if the β(III) and γ phases, respectively, were totally and exclusively formed during the charge (one electron per Ni atom is expected for the β(III)-phase formation compared to about 1.5 electrons for the γ-phase one). The two lines are superimposed (mixed dashed-dotted line) for charge duration lower than 300 min because the two corresponding behaviours lead to the same NEE values in this range.

### 3.2. Test with electrode formation

The capacity curve in Fig. 2, corresponding to the cycling with preliminary electrode formation, follows quite well the theoretical line for charge durations lasting less than 250 min. It exhibits an inflexion point for an NEE close to 0.9 electron and a charge duration of 270 min. This point separates the experimental curve into two distinct domains denoted ① (below 270 min) and ② (above 270 min) in the figure. The discharge derivative curves in Fig. 4(d) for charge durations below 270 min (i.e. corresponding to domain ① in Fig. 2) exhibit a very wide peak characteristic of the β(II)/β(III) system, without any contribution at low potential that would indicate the presence of the α/γ system. Since only the first plateau is involved in the discharge, which is carried out down to 0.9 V, the NEE values reaches only 0.9 instead of 1 as theoretically expected.

The fact that the curve obtained after formation, is located slightly above the theoretical curve in domain ①, may appear surprising at first sight because, at the scale of one cycle, the NEE in discharge cannot theoretically exceed the NEE exchanged during the previous charge. One can assume that during the electrode formation in 1 M KOH, the whole material is not reduced at each discharge, due to the weaker ionic conductivity in low concentrated electrolyte. The presence of residual oxidised material leads, therefore, to

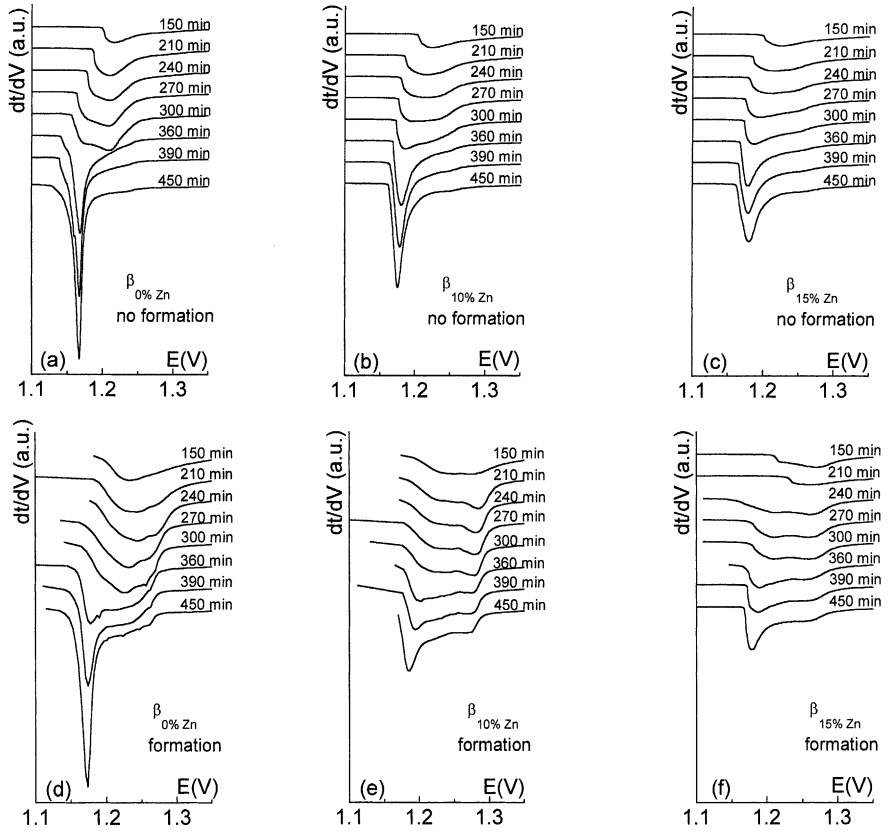


Fig. 4. Overview of the evolution of the discharge derivative curves, as a function of charge duration, for the $\beta_{0\%\ Zn}$, $\beta_{10\%\ Zn}$ and $\beta_{15\%\ Zn}$ phases, galvanostatically tested without ((a)–(c)) or with ((d)–(f)) preliminary electrode formation.

a larger capacity in the very first cycles of the cycling in 8 M electrolyte.

The experimental curve shape in domain ② suggests the involvement of a significant amount of α/γ. This is in accordance with the discharge derivative curves in Fig. 4(d), which, for a charge duration of 300 min, show the appearance of a shoulder around 1.19 V, characteristic of the α/γ system. For increasing charge durations above 300 min, this peak strongly increases in intensity at the expense of the wide contribution, at higher potential, due to the β(II)/β(III) system and becomes predominant for the highest charge durations (390 and 450 min).

It should be noted that the slope of the NEE versus charge duration curve in domain ② is lower than that of the theoretical curve corresponding to the α/γ system (dashed line). This discrepancy may be attributed to the partial presence of β(II)/β(III) in addition to α/γ, which limits the capacity, and to the non-faradic character of the system as a result of the competition between the effective charge and the oxidation of the electrolyte.

### *3.3. Test without electrode formation*

Concerning the experiments without preliminary formation (Fig. 2), the monotonous shape of the experimental curve looks like that of the α/γ theoretical curve, in spite of a shift in NEE to lower values, which suggests that the γ-phase is formed all along the test in this case. This assumption is confirmed by the peculiar shape of the discharge derivative curves (Fig. 4(a)), which shows the contribution of the α/γ system at low potential, even for short charge durations. The peak characterising the α/γ system appears clearly as a shoulder from 270 min of charge onward, the contribution of this system becoming very strong from 360 min onward. The presence of the γ-phase after charge throughout the test is due to the fact that only a fraction of the material works, as a result of the absence of preliminary electrode formation. The activated fraction of the material is indeed locally subject to high charge rates, which favours the formation of the γ-phase. This behaviour, related to the spatial distribution of the material within the electrode, leading to the formation of the γ-phase in the vicinity of the current collector, has been previously discussed by several authors [14,16].

For charge durations lower than 270 min, the involvement in the redox process of only a fraction of the material within the non-preliminary formed electrode, accounts for the lower capacity obtained as compared to the theoretical values (mixed dashed-dotted line), as well as to the capacity obtained after electrode formation (Fig. 2). It can also be assumed that, even for lower charge durations, a significant part of the capacity is lost on charge, due to electrolyte

oxidation. The increase of the working fraction of the initially non-activated material during cycling leads to a decrease in the discrepancy between the curve corresponding to the absence of formation and the two other ones. From 270 min onward, the material activation progresses and the curves corresponding to the test, with or without formation, are almost superimposed.

### 3.4. Influence of the zinc amount

The variations of the NEE, as a function of charge duration, for materials containing various zinc amounts, gathered in Fig. 3(a) and (b) for the test without and with electrode formation, respectively, will be discussed in relation with the corresponding discharge curve derivatives (Fig. 4). In order to highlight the effect of zinc, some curves corresponding to $\beta_{0\%\ Zn}$ and $\beta_{10\%\ Zn}$ were extracted from Fig. 4 and reported in Fig. 5. This allows a more precise comparison of the curve shapes obtained without and with formation for four different charge durations (240, 300, 360 and 450 min).

#### 3.4.1. Preliminary remark

An accurate comparison of Fig. 3(a) and (b) shows that, for charge durations higher than 250 min, the relative location of the curves (versus one another) corresponding to the $\beta_{0\%\ Zn}$, $\beta_{10\%\ Zn}$ and $\beta_{15\%\ Zn}$ phases, is not exactly the same for the tests with formation (Fig. 3(b)) and the tests without formation (Fig. 3(a)). Such small discrepancies and inversions between the curves can be due to the uncontrolled loss of zinc into the electrolyte during the initial formation step. Indeed, previous studies have shown that β(II)-type zinc-substituted nickel hydroxides slowly undergo an Oswald ripening process in KOH solutions. During this reaction (dissolution, re-precipitation and growth), a significant part of zinc is lost in the solution [10]. This reaction occurs simultaneously with the redox processes which mainly involve solid state reactions. The materials after formation, therefore, contain a zinc amount lower than the pristine one; moreover, the kinetics of zinc loss (related to that of material dissolution) is likely to be different depending on the zinc amount.

From a general point of view, the tendencies deduced in the case of the non-substituted β(II)-phase from the comparison of the cycling tests, with and without preliminary electrode formation (Section 3.4), prove quite similar for the zinc-substituted materials. One of the main results is that the ratio of γ to β(III) phases amounts, formed in charge for a given charge duration, remains consistently higher for the non-preliminarily-formed electrode than for the formed one, whatever the substituted zinc amount. This leads to a higher capacity when the non-formed electrode is overcharged (Fig. 3). This behaviour is clearly underlined in Fig. 5 for charge durations of 240, 300 and 360 min, the contribution to the total capacity of the peak at low potential, due to α/γ, being larger for each material tested without formation, than

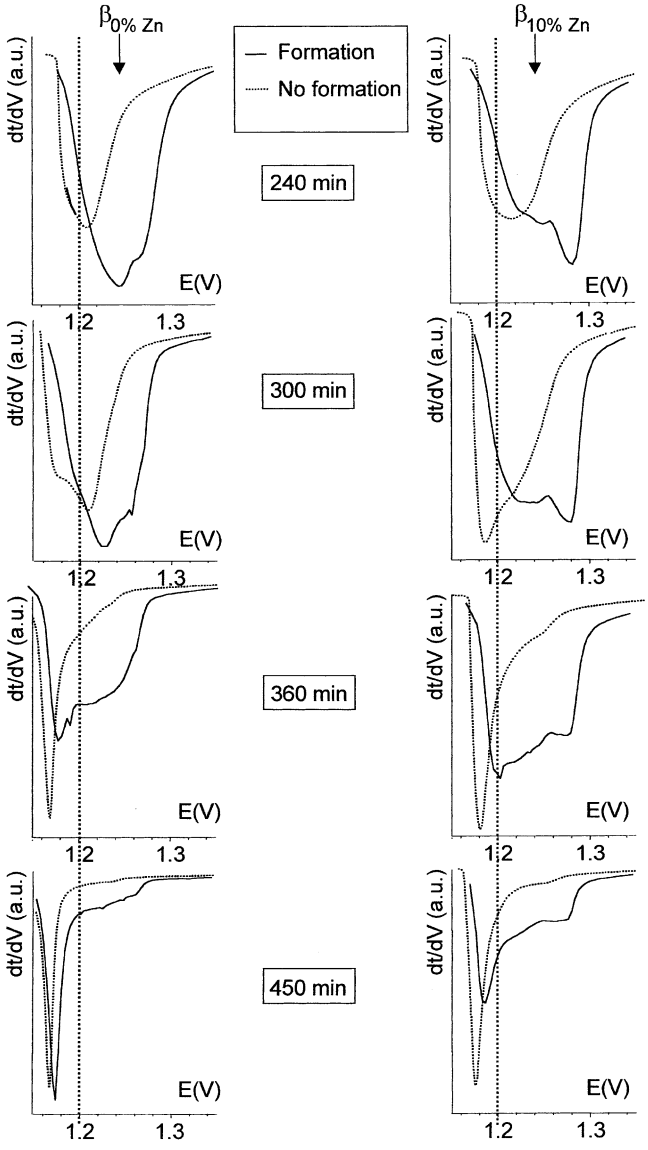


Fig. 5. Comparison of the shapes of the discharge derivative curves, obtained during efficiency tests, performed without or with preliminary electrode formation, for charge durations of 240, 300 360 and 450 min, in the case of the $\beta_{0\%\ Zn}$ and $\beta_{10\%\ Zn}$ phases.

for the same material tested with formation. For a 450 min charge duration, this difference, though still present, is attenuated, since the long charge duration tends to favour the formation of γ in charge.

These results show that it is reasonable to consider the electrochemical behaviour of the formed electrode in order to discuss the effect of zinc. Only the data corresponding to the formed electrode will, therefore, be considered in the following. For charge durations up to 240 min, no significant tendency versus the zinc amount can be deduced, neither from the capacity curves (Fig. 3(b)), nor from the discharge derivative curves (Fig. 5). The capacity curves for various zinc amounts are very close to one another and unable to be distinguished. The evolution of the discharge derivative curves in this charge duration domain are also difficult to

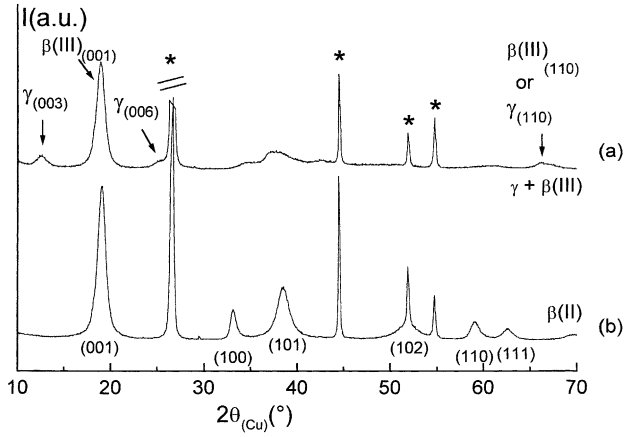


Fig. 6. XRD patterns of electrodes with $\beta_{10\%\ Zn}$ as the active material, recovered in the charged (a) and discharged (b) state, after an efficiency test with a preliminary electrode formation. Stars show the diffraction lines of Ni and C added to the electroactive material.

accurately comment upon, because they correspond to very incomplete discharges.

For charge durations higher than 250 min, the capacity curves show a decrease in their slope, this trend being more and more accentuated as the zinc amount increases (Fig. 3(b)). This peculiar curve shape suggests that the amount of γ-phase formed in charge decreases in favour of the β(III)-phase with an increasing zinc amount. This evolution follows the general trend highlighted by the discharge derivative curves ($\beta_{0\%\ Zn}$ and $\beta_{10\%\ Zn}$), that is to say a decrease in intensity of the low potential peak of α/γ in favour of the wide contribution, at higher potential, assigned to β(II)/β(III) (Figs. 4 and 5). Fig. 6 shows XRD patterns of an electrode with $\beta_{10\%\ Zn}$ as the active material, which was recovered in the charged (a) and discharged (b) state, at the end of an efficiency test with preliminary formation. A mixture of γ and β(III) phases is obtained after charge, which confirms the involvement of both the α/γ and β(II)/β(III) systems, as highlighted by the derivative curves for the 450 min charge (Figs. 4 and 5). In this mixture, the β(III)-phase is largely predominant, in agreement with the shape of the derivative curves. After discharge, a β(II)-phase is obtained. It results from the reduction of the β(III)-phase, but also indirectly from the γ-phase, which is reduced to an α-phase, this phase being in turn transformed into a β(II)-phase. These results clearly confirm the inhibition of the α/γ system, in agreement with literature [1–7,11]. In the latter work [11], this inhibition was supposed to be due to the presence of zinc cations in tetrahedral sites in the interslab space of the β(II) phases, obtained during electrochemical cycling as a result of an Oswald ripening of the reduced material.

### 3.5. Effect on the cell voltage

Zinc has also been reported by several authors to increase the cell voltage [17–20]. In order to attempt to visualise this effect, a vertical dashed line was drawn on each derivative curve of Fig. 5. This line corresponds to the 1.2 V value, which is an average discharge voltage in commercial alkaline batteries. Typically in all experiments, when the amount of zinc increases from 0 to 10%, the area under the curve part above 1.2 V increases at the expense of the area below this value. This study confirms that zinc tends to increase the cell voltage.

Several years ago we proposed a model in order to explain the effect of the substituting cations on the cell voltage of alkaline and lithium batteries, with nickel hydroxide or $LiNiO_2$ derivatives, respectively, as positive electrode materials [21]. This model, which is based on the difference in size between the substituting cation and nickel, explains quite well the observed effect of all substituting cations, except for aluminium. It is considered that the substitution of a cation, larger than nickel, tends to increase the size of the $NiO_6$ octahedra via a co-operative effect, making nickel oxidation more difficult, and therefore, increasing the cell voltage. This behaviour is very clearly evidenced by Mössbauer spectroscopy studies of iron-substituted nickel hydroxides and iron nickelates [22–25]. The opposite effect is observed when a cation which is smaller than nickel ($Co^{3+}$) is substituted. In the case of aluminium, an hypothesis, based on the hybridisation of metal–oxygen atomic orbitals, was recently proposed to explain the experimental increase of the cell voltage in the $LiCo_{1-y}Al_yO_2$ layered system [26]. In the case of zinc-substituted nickel hydroxide, the large size of $Zn^{2+}$ cations versus $Ni^{2+}$ ones makes nickel oxidation more difficult in charge and tends to facilitate the nickel reduction in discharge. This behaviour tends to increase the cell voltage. Moreover, we have shown that octahedral vacancies are formed in the slab as a result of the removal of a part of the zinc within the solid state, during electrochemical cycling. The presence of cationic vacancies within the slab can also be assumed to increase the slab thickness, and therefore, plays the same role as a large substituting cation. Moreover, the average oxidation state of nickel must increase to compensate for the existence of cationic vacancies, thus further contributing to an increase of the cell voltage.

## 4. Conclusion

During efficiency tests starting from β(II)-type nickel hydroxides containing zinc, partially substituted for nickel, the absence of a preliminary electrochemical formation of the electrode in a low-concentrated electrolyte, leads to the formation of a higher amount of γ-phase on charge than after an electrode formation. This effect is due to the poor activation of the material resulting in local high rate overcharge, whatever the cycling conditions. An increase of the zinc amount in the starting materials tends to prevent the formation of the γ-phase from the β(III) one and to increase the cell voltage. Even if a significant part of zinc is

lost in the electrolyte during the cell cycling, the effects of zinc on the behaviour of the nickel hydroxide electrode still remain. It can be assumed that this behaviour results from some reactions occurring within the solid state.

One question remains open concerning the effects of zinc, added to the electrolyte, on the positive electrode behaviour. A study aiming at clarifying this point is being carried out.

## Acknowledgements

The authors are grateful to M. Ménétrier, P. Bernard and J.M. Dauchier for fruitful discussion, M. Basterreix for technical assistance and to SAFT, ANRT and Région Aquitaine for financial support.

## References

[1] B.B. Ezhov, O.G. Malandin, J. Electrochem. Soc. 138 (1991) 885.
[2] M. Oshitani, K. Takashima, Y. Matsumara, in: D.A. Corrigan, A.H. Zimmerman (Eds.), Proceedings of the Symposium on Nickel Hydroxyde Electrodes, Electrochem. Soc. Proc. Ser. 4 (1990) 197.
[3] M. Oshitani, T. Takayama, K. Takashima, S. Tsuji, J. Appl. Electrochem. 16 (1986) 403.
[4] M. Oshitani, M. Watada, T. Tanaka, T. Iida, Electrochem. Soc. Proc. Ser. 27 (1994) 303.
[5] M. Oshitani, H. Yufu, K. Hasegawa, Yuasa Battery Co. Ltd., European Patent 89,303,952.9 (1989).
[6] D.H. Fritts, The nickel electrode, in: R.G. Gunther, S. Gross (Eds.), Electrochem. Soc. Proc. Ser. 4 (1982) 175.
[7] A. Yuan, S. Cheng, J. Zhang, C. Cao, J. Power Sources 77 (1999) 178.
[8] C. Tessier, L. Guerlou-Demourgues, C. Faure, A. Demourgues, C. Delmas, J. Mater. Chem. 10 (2000) 1185.
[9] W. Oswald, Z. Phys. Chem. 34 (1900) 495.
[10] C. Tessier, L. Guerlou-Demourgues, C. Faure, M. Basterreix, G. Nabias, C. Delmas, Solid State Ionics 133 (2000) 11.
[11] C. Tessier, C. Faure, L. Guerlou-Demourgues, C. Denage, G. Nabias, C. Delmas, J. Electrochem. Soc., submitted for publication.
[12] C. Tessier, P.H. Haumesser, P. Bernard, C. Delmas, J. Electrochem. Soc. 146 (1999) 2059.
[13] L. Guerlou-Demourgues, C. Delmas, J. Electrochem. Soc. 143 (1996) 561.
[14] N. Sac-Epée, M.R. Palacin, B. Beaudoin, A. Delahaye-Vidal, T. Jamin, Y. Chabre, J.M. Tarascon, J. Electrochem. Soc. 144 (1997) 3896.
[15] R. Barnard, C.F. Randell, F.L. Tye, J. Appl. Electrochem. 10 (1980) 109.
[16] R.A. Huggins, H. Prinz, M. Wohlfahrt-Mehrens, L. Jörissen, W. Witschel, Solid State Ionics 70/71 (1994) 417.
[17] R.J. Doran, in: Proceedings of the International Symposium on Batteries, Paper y, Royal Aircraft Establishment, Farnborough, UK, 1958.
[18] D.A. Corrigan, R.M. Bendert, J. Electrochem. Soc. 136 (1989) 723.
[19] M.E. Unates, M.E. Folquer, J.R. Vilche, A.J. Arvia, J. Electrochem. Soc. 135 (1988) 25.
[20] M.E. Unates, M.E. Folquer, J.R. Vilche, A.J. Arvia, in: D.A. Corrigan, A.H. Zimmerman (Eds.), Proceedings of the Symposium on Nickel Hydroxide Electrodes, Electrochem. Soc. Proc. Ser. 4 (1990) 134.
[21] C. Delmas, Solid state ionics III, in: G.A. Nazri, J.M. Tarascon, M. Armand (Eds.), Mater. Res. Soc. 293 (1993) 15.
[22] L. Demourgues-Guerlou, L. Fournès, C. Delmas, J. Solid State Chem. 114 (1995) 6.
[23] L. Guerlou-Demourgues, L. Fournès, C. Delmas, J. Electrochem. Soc. 143 (1996) 3083.
[24] C. Delmas, G. Prado, A. Rougier, E. Suard, L. Fournès, Solid State Ionics 135 (2000) 71.
[25] G. Prado, A. Rougier, L. Fournès, C. Delmas, J. Electrochem. Soc. 147 (2000) 2880.
[26] G. Ceder, Y.M. Chiang, D.R. Sadoway, M.K. Aydinol, Y.I. Jang, B. Huang, Nature 392 (1998) 684.